Lawrence Berkeley National Laboratory
Recent Work

Title

Ceramic Microstructures and Their Elucidation by Imaging, Diffraction and Spectroscopic Methods

Permalink

https://escholarship.org/uc/item/8pw3n70m

Author

Krishnan, K.M.

Publication Date

1992-02-01

eScholarship.org Powered by the California Digital Library
University of California

LBL-32002
UC-404

Lawrence Berkeley Laboratory
UNIVERSITY OF CALIFORNIA

Materials Sciences Division

National Center for Electron Microscopy

To be presented at the Tenth EUREM Conference, Granada, Spain, September 7–11, 1992, and to be published in the Proceedings

Ceramic Microstructures and Their Elucidation by Imaging, Diffraction and Spectroscopic Methods

K.M. Kirshnan

February 1992

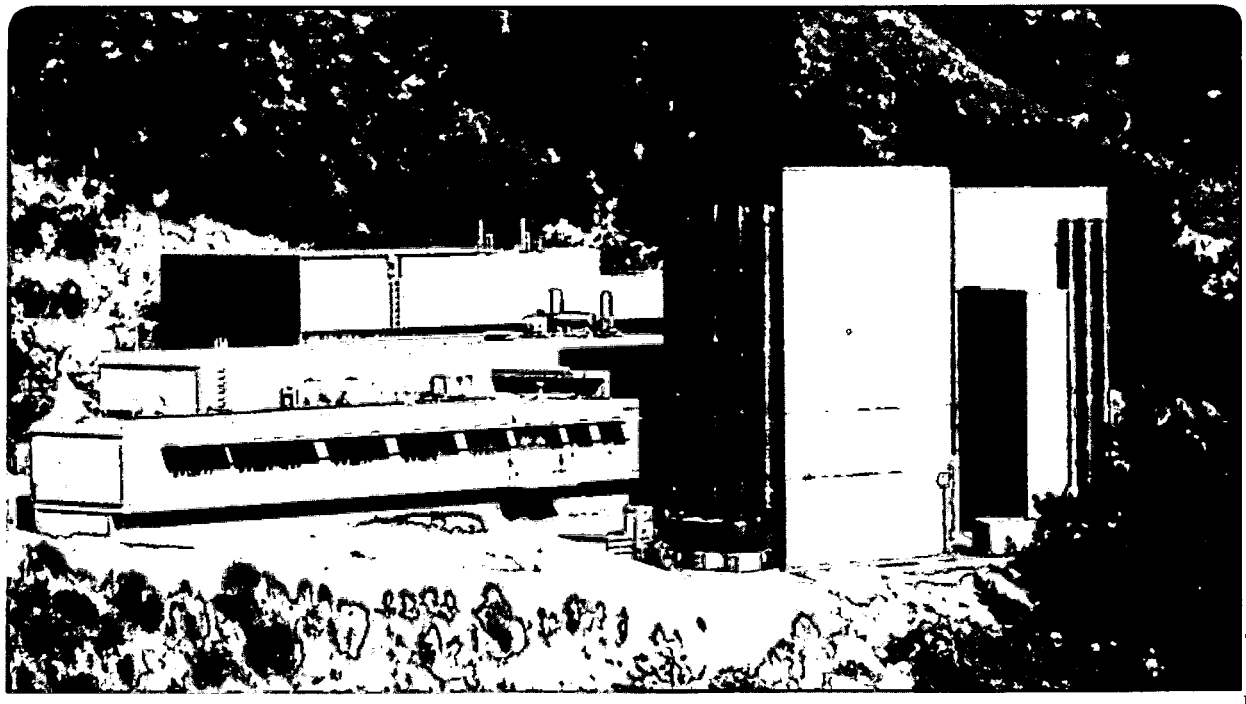

Prepared for the U.S. Department of Energy under Contract Number DE-AC03-76SF00098

LBL-32002
Copy 2
| LOAN COPY |
|Circulates |
|for 4 weeks| Bldg. 50 Library.

DISCLAIMER

This document was prepared as an account of work sponsored by the United States Government. Neither the United States Government nor any agency thereof, nor The Regents of the University of California, nor any of their employees, makes any warranty, express or implied, or assumes any legal liability or responsibility for the accuracy, completeness, or usefulness of any information, apparatus, product, or process disclosed, or represents that its use would not infringe privately owned rights. Reference herein to any specific commercial product, process, or service by its trade name, trademark, manufacturer, or otherwise, does not necessarily constitute or imply its endorsement, recommendation, or favoring by the United States Government or any agency thereof, or The Regents of the University of California. The views and opinions of authors expressed herein do not necessarily state or reflect those of the United States Government or any agency thereof or The Regents of the University of California and shall not be used for advertising or product endorsement purposes.

Lawrence Berkeley Laboratory is an equal opportunity employer.

DISCLAIMER

This document was prepared as an account of work sponsored by the United States Government. While this document is believed to contain correct information, neither the United States Government nor any agency thereof, nor the Regents of the University of California, nor any of their employees, makes any warranty, express or implied, or assumes any legal responsibility for the accuracy, completeness, or usefulness of any information, apparatus, product, or process disclosed, or represents that its use would not infringe privately owned rights. Reference herein to any specific commercial product, process, or service by its trade name, trademark, manufacturer, or otherwise, does not necessarily constitute or imply its endorsement, recommendation, or favoring by the United States Government or any agency thereof, or the Regents of the University of California. The views and opinions of authors expressed herein do not necessarily state or reflect those of the United States Government or any agency thereof or the Regents of the University of California.

LBL-32002

Ceramic Microstructures and Their Elucidation by Imaging, Diffraction and Spectroscopic Methods

K.M. Krishnan

Materials Science Division
National Center for Electron Microscopy
Lawrence Berkeley Laboratory
University of California, Berkeley, CA 94720

Presented at the 10th EUREM Conference
Granada, Spain
7-11 Sept. 1992

This work was supported in part by the Director, Office of Energy Research, Office of Basic Energy Sciences, Materials Science Division of the U.S. Department of Energy under Contract No. DE-AC03-76SF00098.

CERAMIC MICROSTRUCTURES AND THEIR ELUCIDATION BY IMAGING, DIFFRACTION AND SPECTROSCOPIC METHODS.

Kannan M. Krishnan

Materials Sciences Division, National Center for Electron Microscopy, Lawrence Berkeley Laboratory, 1 Cyclotron Road, Berkeley, CA 94720.

The development and potential utilization of ceramic materials is dependent on a systematic effort involving processing, characterization and appropriate property measurements. The methods of characterization are numerous and it is important to employ the one that is appropriate to the problem both in terms of its information content and the achievable level of resolution. With the incorporation of fine probe forming capabilities in a transmission electron microscope and the development of related diffraction, imaging and spectroscopic methods, it is now possible to obtain structural and chemical information from the same region of the sample at high spatial resolution. In this review, recent advances along with representative examples in the application of high resolution electron microscopy (HREM), convergent beam electron diffraction (CBED), low atomic number element microanalysis by x-ray emission spectroscopy (XES), fine structures in electron energy-loss spectroscopy (EELS) and specific site occupancy determination by channelling experiments are discussed.

ALUMINIUM OXYNITRIDE CERAMICS: Pure single crystal aluminium oxide is an anisotropic material and exhibits directional variation in optical and thermal properties. True optical transparency of polycrystalline Al_2O_3 is impossible unless all the grains are identically oriented. An alternative but simpler approach is the stabilization of cubic Al_2O_3 by the addition of nitrogen, in the form of AlN, to form defective spinels. Based on the relatively wide range of compositional stability[1], roughly centered at 35.7 mol% AlN, fully dense materials were sintered for microstructural evaluation. Comparing the symmetries (figure 1) of the whole pattern (4mm), the central transmitted disc (4mm) and the (400) dark field order when set at the Bragg condition (2mm), with the tables of Buxton et al [2], it can be concluded that this material has a projected diffraction group of $4mm1_R$ and a point group of m3m. The displacements of the position of the FOLZ discs with respect to the ZOLZ disc confirms that the material is indeed face centered cubic with a spinel structure. Unfortunately, most AlN powders contain some oxygen impurities and therefore such sintering processes result in materials with polytype-like phases of AlN [3]. The periodicity of the faulting, that defines the character of this modulated structure, is a function of the overall composition and constrained by charge balance. Figure 2 shows a SAD pattern, conventional lattice image and an optical diffractogram from a region of the 32H polytypoid structure. The position of the (010) spot with respect to the transmitted beam in the SAD confirms the hexagonal stacking sequence. From this SAD pattern, the repeat distance along the c-axis can be calculated to be 8.3nm for this structure. However, both the lattice

image and the accompanying optical diffractogram show a spacing of 4.3nm. This is not a surprising discrepancy, for the nH polytypoids in this system normally consist of two blocks of n/2 layers related by a c-glide plane. This is verified in figure 3, which shows a CBED pattern obtained with a 60nm diameter probe (information is averaged over a few unit cells) oriented such that the c-axis is parallel to the incident beam. From the radius of the FOLZ ring, the periodicity along the c-axis is calculated to be 4.2nm. If these polytypoids are compositionally stabilized, it is predicted that the anion/cation ratio should be 17/16 or 1.06. A typical EDX spectrum obtained from a 32H region of the sample (figure 4) analyzed by using experimentally measured K-factors [4,5], confirms a composition of 47.9 at.% Al, 13.8 at.% O and 38.3 at.% N with an experimental error of ± 2 %. The anion/cation ratio obtained from this measurement, i.e. 1.08, agrees well with the predicted value, confirming the stability of such a long period polytypoid. However, if direct imaging of the structure with atomic resolution is used (figure 5), the periodicity along the c-direction can be shown to be a sequence of alternate 7:9:7:9 ... repeats. This result can be interpreted as parallel intergrowths of the 27R (c = 7.2 nm) and 21R (c = 5.7 nm) polytypoids. Clearly adjacent units of 21R and 27R add up to the 32H repeat units. A detailed interpretation of these images would require simulations of the image based on a predicted intergrowth structure.

NOVEL GRAPHITES: A novel graphite material, BC_3, has been synthesized by the interaction of benzene and boron trichloride at 800 °C. These reactions: $2\ BCl_3 + C_6H_6 \rightarrow 2\ BC_3 + 6\ HCl$, are driven by favourable TDS values associated with HCl elimination. For BC_3, an ordered structure with periodic substitution of B for every other C in the graphite lattice has been suggested. Recently, important differences in the density of states (DOS) of BC_3 from graphite, for the proposed structure has been suggested[6]. Two sharp peaks in the DOS associated with the p band below the conducting s bands(figure 6a), unlike graphite with one peak, are predicted. Representative K-edge spectra of B and C obtained from a thin foil of BC_3 are shown in figure 6b. The fine structrure of the B K-edge shows two sharp peaks at 187.5eV and 190.1eV. These peaks can be assigned to the excitation of the 1s electrons to unoccupied levels in the conduction band. Observation of these features provides direct confirmation for the atomic arrangement in this material [7].

IRON OXIDES: The ability to resolve the oxidation state and the coordination of iron in various spinels is important in understanding the magnetic behaviour of a wide range of magnetic oxides. Four different model oxide mineral sample, each containing iron in a specific oxidation state and coordination, were investigated. They were franklinite (nominal composition $[Zn,Mn]Fe^{3+}{}_2O_4$) where Fe(III) is in octahedral sites; hercynite (nominal composition $Fe^{2+}Al_2O_4$) where Fe(II) is in tetrahedral sites; fayalite (nominal composition Fe_2SiO_4) where Fe(II) is in octahedral coordination; and an iron analogue of leucite (nominal composition $KFeSi_2O_6$) where Fe(III) is in tetrahedral coordination. Figures 7a and b show the L_3/L_2 edges for Fe(III) in octahedral and tetrahedral coordination respectively. In the former case, both the L_3 and L_2 edges show distinct splittings, separated by 1.6eV, at the onset of the edge. No such splitting is observed in the latter. For Fe(II) in

octahedral and tetrahedral sites, the L_3/L_2 peak height ratio is lower when compared to Fe(III). The observed fine structures can be interpreted in terms of a simple ligand field approach using the commonly observed low spin state for iron[8]. For Fe(III) in octahedral coordination, in addition to the empty e_g levels there is an unpaired electron in the t_{2g} level. This explains the splitting of the L_3 and L_2 white line features in Figure 7a. For Fe(III) in tetrahedral coordination, the energies of the ligand field split levels, e_2 and t_2, are reversed. The lower e_2 level is completely filled and therefore one observes a single peak (fig.7b).

ATOM LOCATION BY CHANNELLING ENHANCED MICROANALYSIS: For crystalline materials both the characteristic energy-loss edges and x-ray intensities are governed by phenomena that are highly localized at the atomic sites. They show strong dependence on the orientation of the incident beam and this has been developed into a powerful crystallographic technique for specific site occupancy/valence determinations [9]. For the dolomite structure in the [1210] orientation (figure 8) when the (0001) systematic row is excited the wave field of the dynamically diffracted electrons in the crystal is two-dimensional, i.e., constant in a direction normal to the c-axis. In this structure, the candidate sites of interest (Mg and Ca) occupy alternating planes at one third the unit cell parameter along the c-axis. For the (0001) systematic row, at orientations corresponding to small positive excitation errors (s>o) (figure 9) of the third order Bragg diffraction condition (3g) an enhancement of the Mg Kα is observed. For negative excitation errors (s<o) an enhancement of the Ca Kα is observed. The impurity Fe Kα intensity follows that of Mg Kα, suggesting similar site occupancy. The exact degree of substitution of the impurity atoms (Fe) can be obtained by an elegant method of ratios with respect to the intensities of the reference elements (Mg & Ca) in the host lattice [9]. Site occupancies in a variety of ceramic materials have been measured using this technique. In the case of EELS, combining these orientation dependence with detectable changes in oxidation states (by the small chemical shifts observed in the onset of the core-loss edges) it is also possible to obtain specific site valence information[10].

A NOTE ON LOW-Z MICROANALYSIS: For the characterization of ceramic materials, improvement in the accuracy of microanalysis of low-z elements is desired. For XES, using an UTW detector best results are obtained using experimentally determined k-factors, accurate measurement of sample thickness and correction for absorption in the specimen [5]. For EELS, comparison of experimentally measured partial cross-sections for four different scattering geometries with theoretical calculations using both the standard hydrogenic model and parametrized Hartree-Slater cross-sections show best agreement when experiments are performed in diffraction mode (image coupling) with the probe convergence angle (0.84 mrad) much smaller than the spectrometer collection angle (6.84 mrad) [11].

REFERENCES

[1] J. W. McCauley and N. D. Corbin, J. Am. Cer. Soc. **62**, 476 (1979).

[2] B. F. Buxton et al, Phil. Trans. Roy. Soc. **A281**, 171 (1976).

[3] K. H. Jack, J. Mat. Sci. **11**, 1135 (1976).

[4] G. Cliff and G. W. Lorimer, J. Micros **103**, 203 (1975).

[5] K. M. Krishnan and C. J. Echer, AEM, D.C. Joy ed, SF Press, 99 (1987).

[6] R. M. Wentzcovitch, M. L. Cohen and S. G. Louie, Phys. Lett. **A131**, 457 (1988).

[7] K. M. Krishnan, App. Phys. Lett. **58**, 1857 (1991).

[8] K. M. Krishnan, Ultramicroscopy, **32**, 309 (1990)

[9] K. M. Krishnan, Scanning Microscopy Supp **4**, 157 (1990).

[10] J. Tafto and O. L. Krivanek, Phys. Rev. Lett. **48**, 560 (1982).

[11] K. M. Krishnan an C. J. Echer, Microbeam Analysis, Ed. D.G. Howitt, SF Press, 259 (1991).

FIGURE CAPTIONS

1. CBED patterns in the <100> orientation confirming the spinel structure of AlON.
2. SAD pattern, lattice image and optical diffractogram from the hexagonal long period 32H polytypoid structure.
3. A CBED pattern in the <0001> orientation for the 32H poytypoid. The structure with c=8.4nm has a glide plane at half the unit cell parameter.
4. XES spectrum with the UTW detector and analysis from 32H.
5. A HREM image of the 32H obtained on the atomic resolution microscope. The 16 layer structure is shown to be an intergrowth of 9 and 7 layer repeats.

6a. Total DOS of a BC_3 monolayer showing the splitting of the p band.

6b. B-K and C-K edges from BC_3 with the C-K edge for graphite superimpose for comparison.

7. L3 and L2 edges for Fe(III) in (a)octahedral and (b)tetrahedral coordination along with the ligand field splitting.
8. Crystallographic structure of dolomite projected along the c-axis.
9. Orientation dependent x-ray emission for dolomite along the [1000] systematic row.

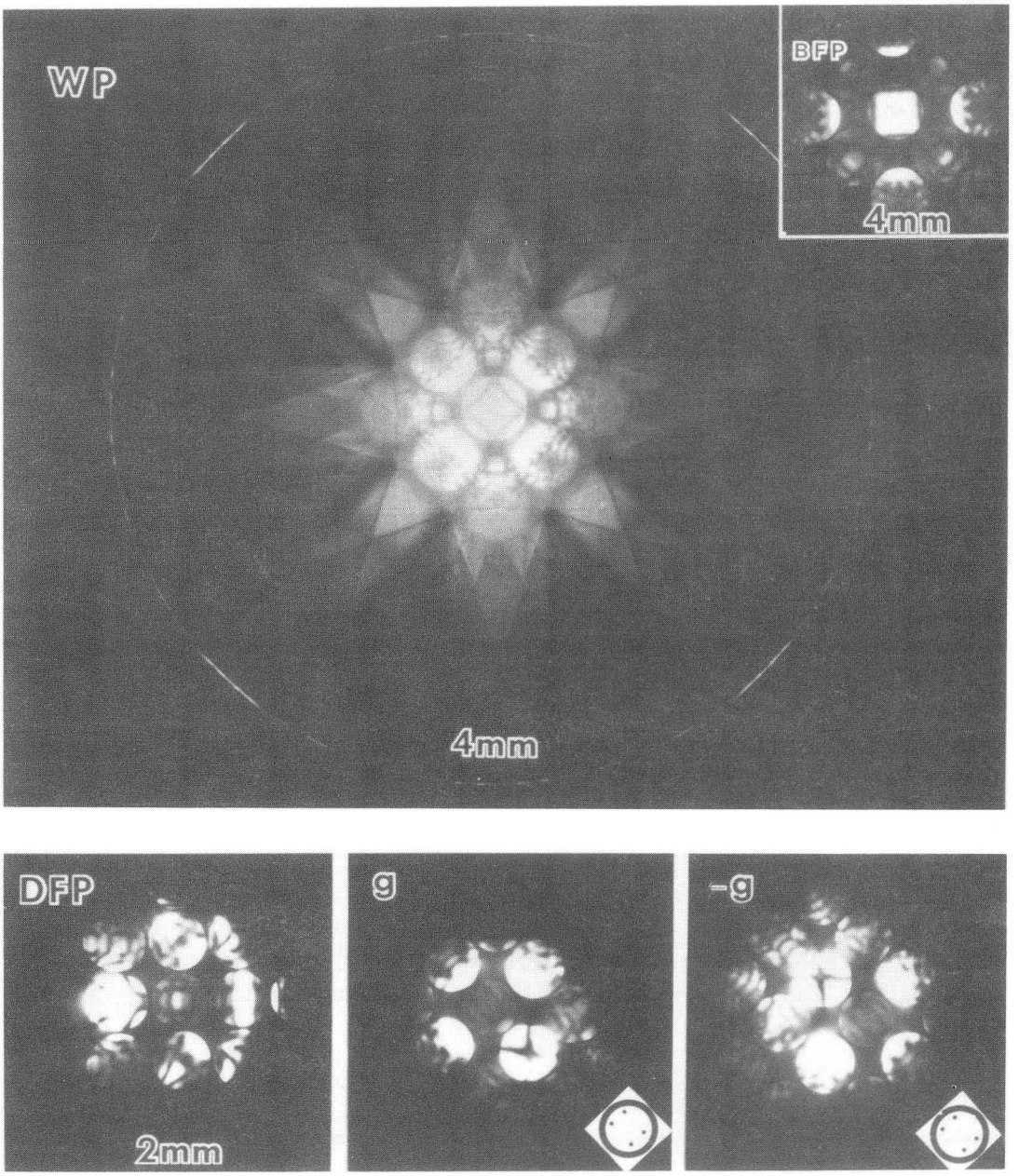

XBB856-4534

Figure 1

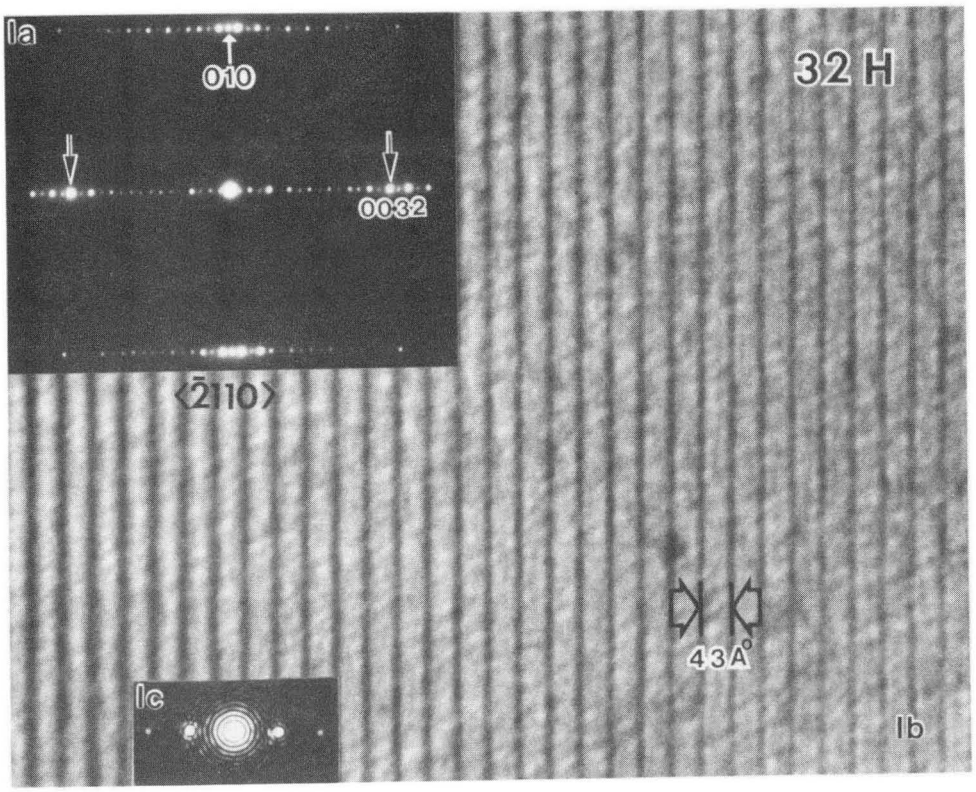

XBB872-1960

Figure 2

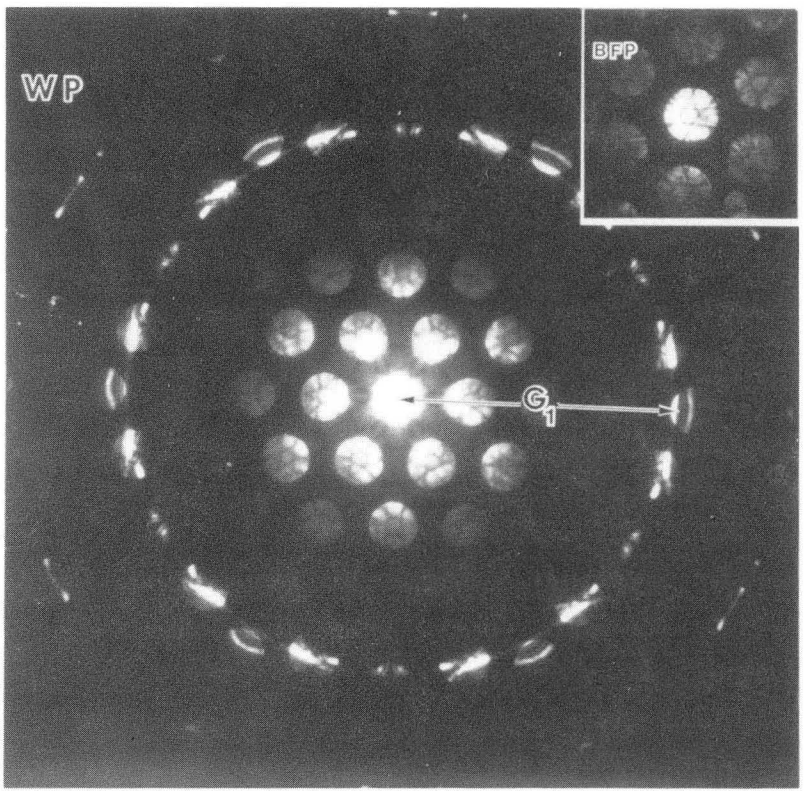

XBB 856-4533

Figure 3

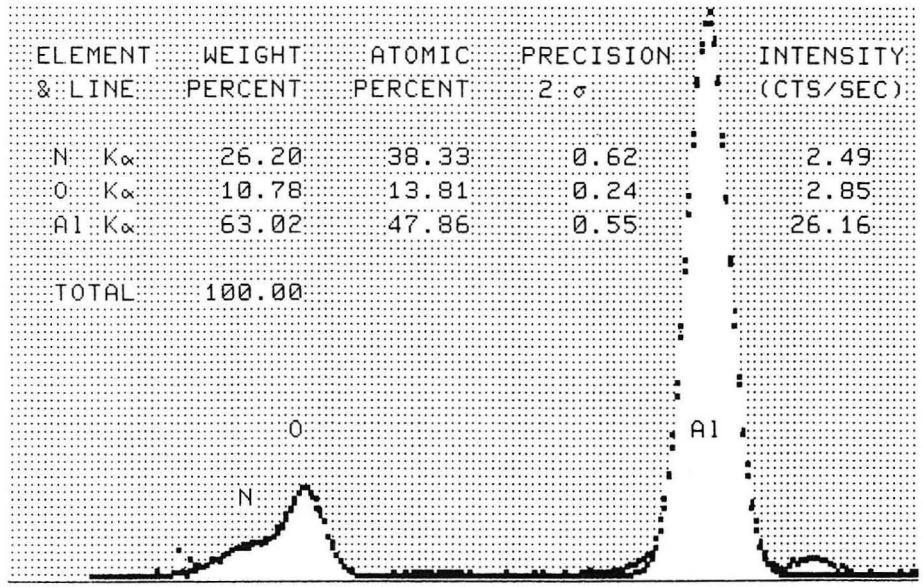

XBL 871-309

Figure 4

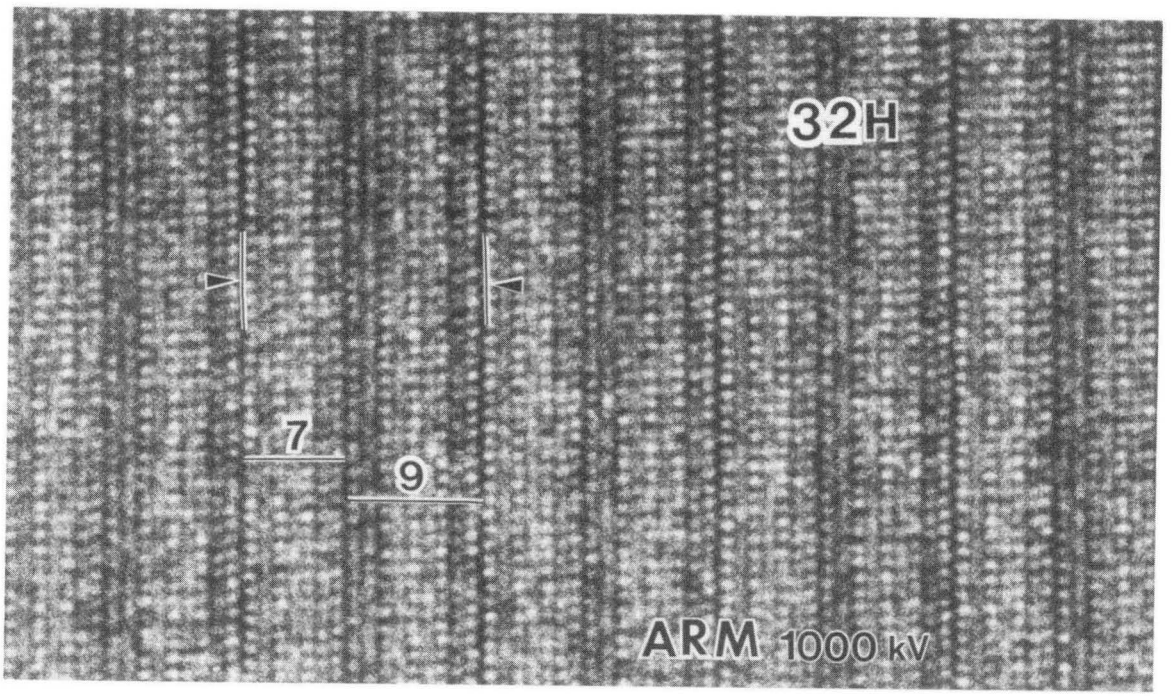

XBB872-959

Figure 5

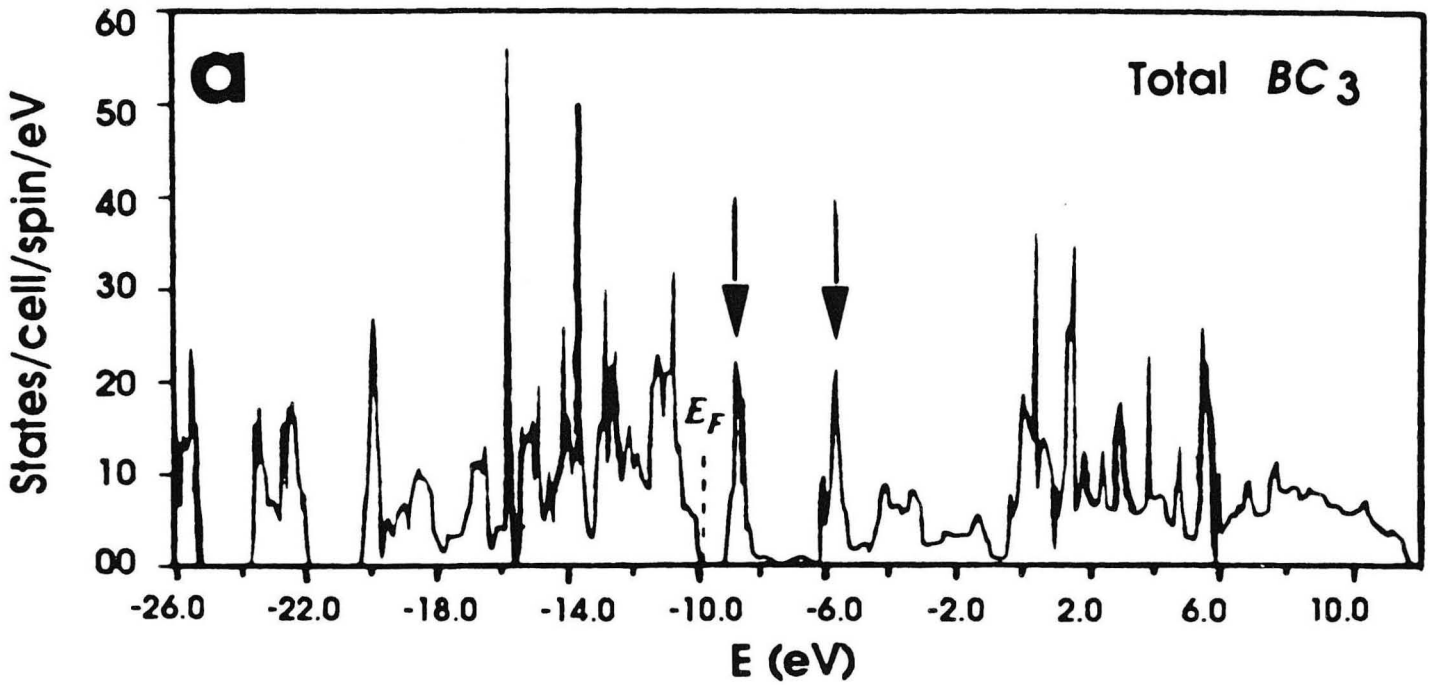
a
Total BC_3
States/cell/spin/eV
60
50
40
30
20
10
00
E_F
-26.0
-22.0
-18.0
-14.0
-10.0
-6.0
-2.0
2.0
6.0
10.0
E (eV)

Figure 6a

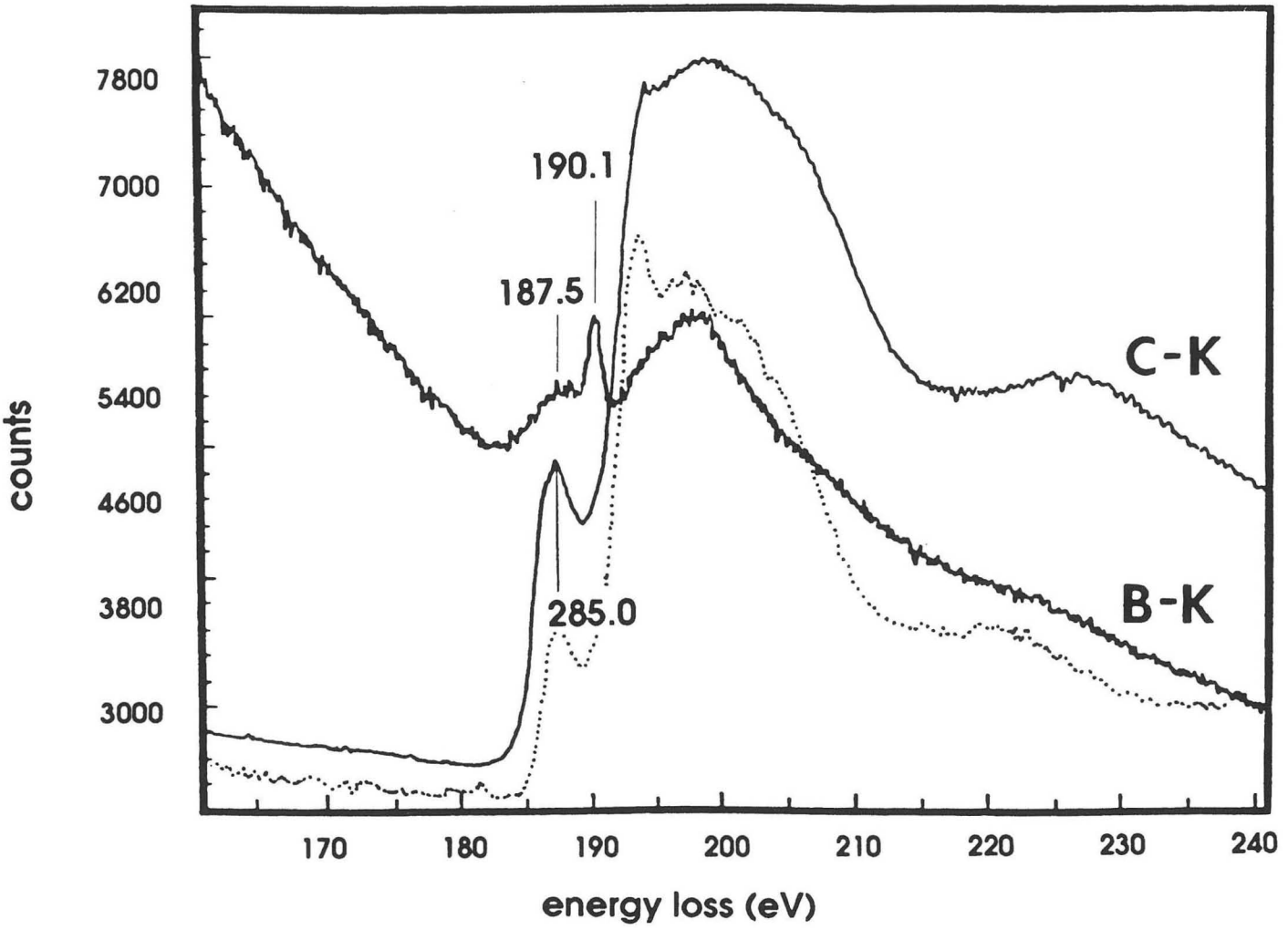

XBL 913-398

Figure 6b

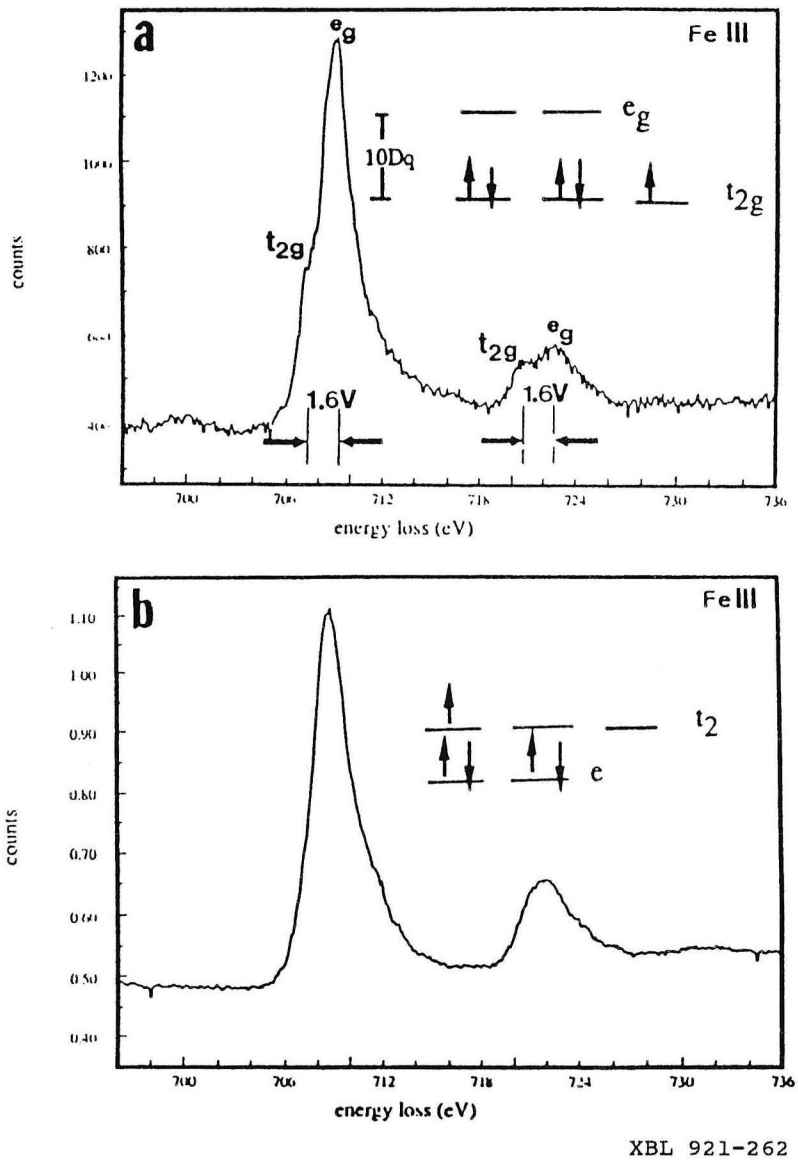
a
Fe III
e_g
10Dq
t_{2g}
e_g
t_{2g}
t_{2g}
e_g
1.6V
1.6V
counts
energy loss (eV)
b
Fe III
t_2
e
counts
energy loss (eV)
XBL 921-262

Figure 7

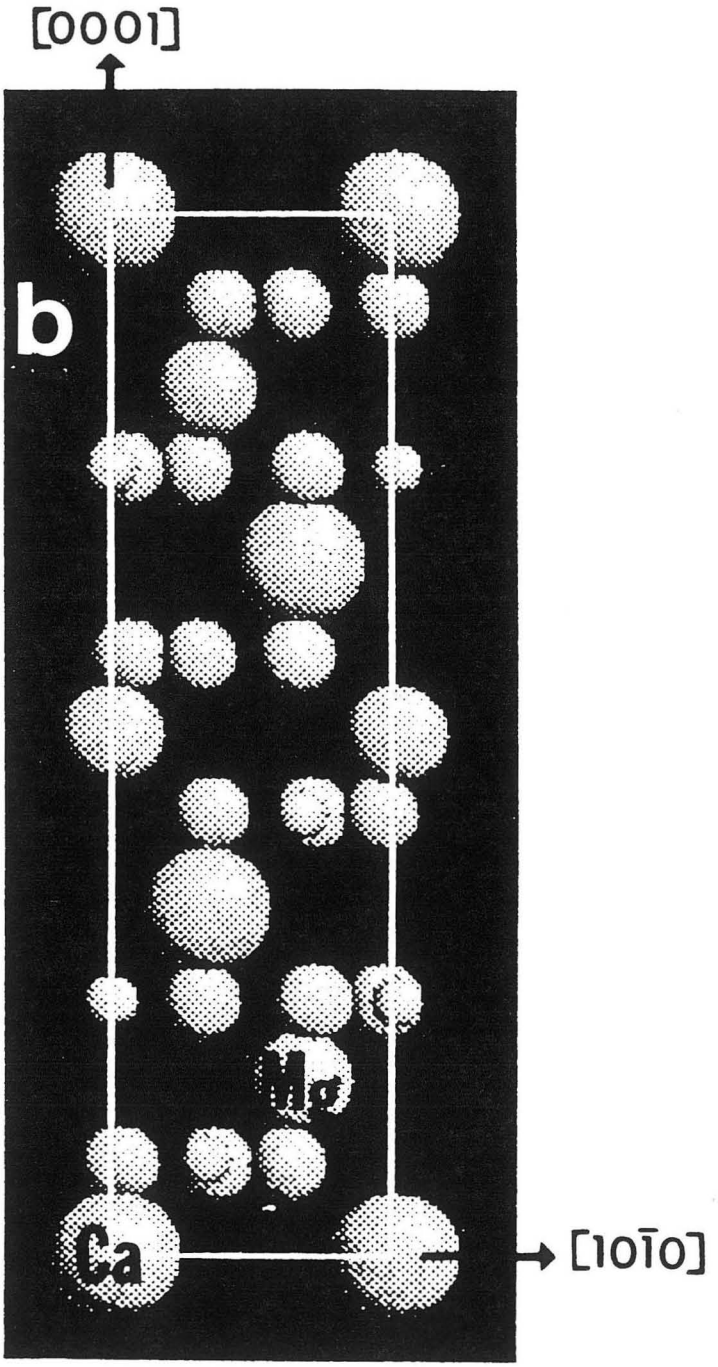

DOLOMITE [11$\bar{2}$0]

XBL 8711-4768 A

Figure 8

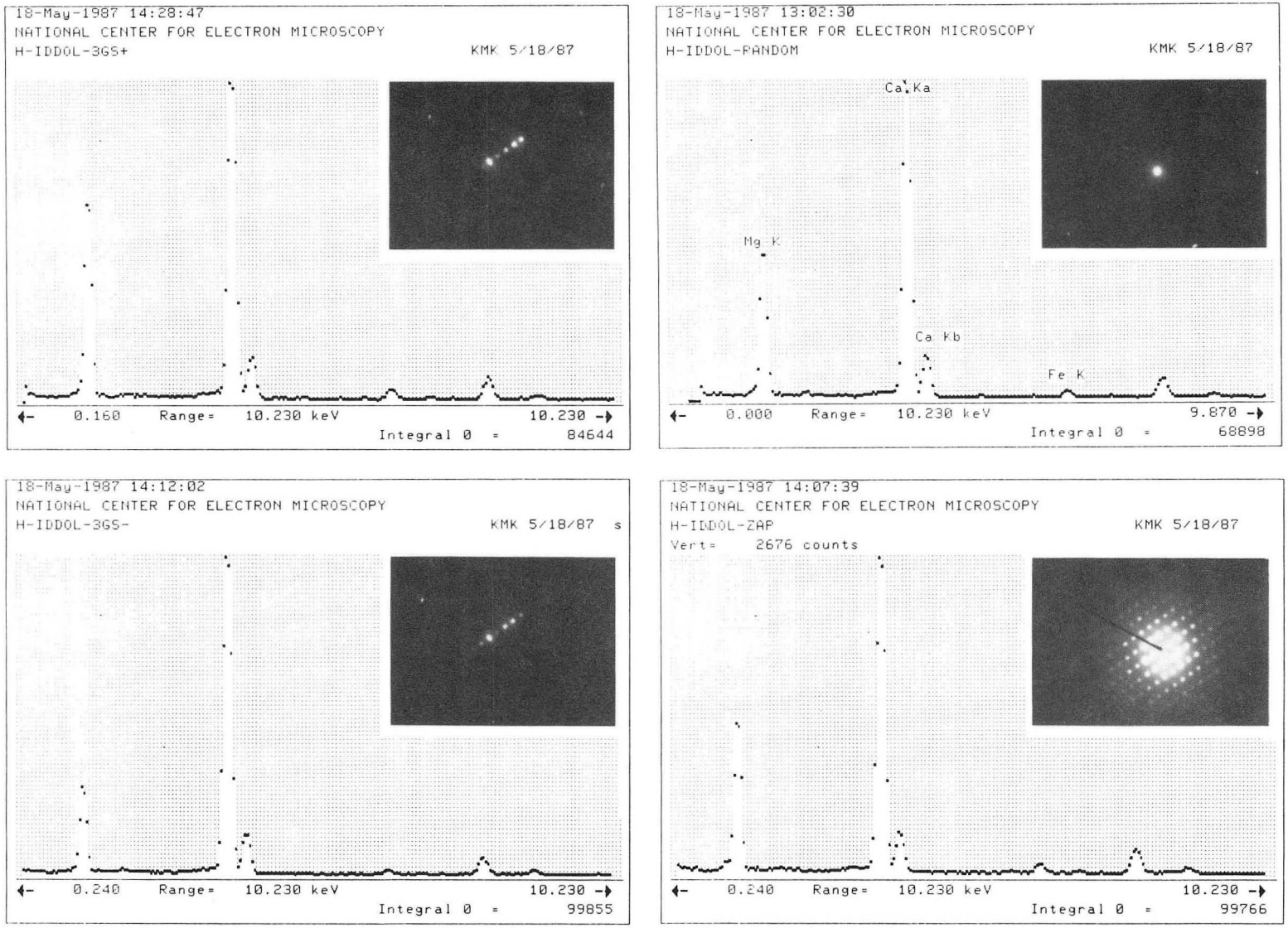

XBB877-5443

Figure 9

LAWRENCE BERKELEY LABORATORY
UNIVERSITY OF CALIFORNIA
TECHNICAL INFORMATION DEPARTMENT
BERKELEY, CALIFORNIA 94720